# On Multistreaming with Compact Antenna Arrays

Michel T. Ivrlač and Josef A. Nossek
Institute for Circuit Theory and Signal Processing
Technische Universität München, D-80333 Munich, Germany
email: {ivrlac, nossek}@tum.de

***Abstract*—We investigate the capability of compact antenna arrays to support the simultaneous transfer of several independent data streams over the same band of frequencies. It is shown that the near-field interaction of the closely spaced antennas inside the arrays accounts for a surprisingly good multistreaming capability, even for extremely compact arrays. This result is demonstrated for the case of a $2 \times 2$ system of thin half-wavelength dipoles in a multipath environment provided by two perfectly conducting reflector plates, and isotropic background noise. Decoupling/power-matching and decoupling/noise-matching networks are applied at the transmit side and the receive side arrays, respectively. The analysis is based on a circuit theoretic multiport model of the system which captures all relevant physics of antenna mutual coupling, the influence of the matching networks, and noise. It is shown that in the absence of heat loss in the matching networks and antenna wires, the simultaneous transfer of two data streams can work perfectly well even as the separation between the antennas inside the arrays approaches zero.**

## I. Introduction

Communication systems which use more than one antenna at both the transmitting and the receiving end of the link (so-called multi-input multi-output (MIMO) systems), potentially support the transfer of several data streams at the same time using the same band of frequencies. In order for this so-called *multistreaming* to work, the propagation channel must allow the transmitted signal to travel to the receiver over a number of sufficiently different paths in space, and arrive there simultaneously from different directions. This spatial structure of the channel can then be exploited by spatial signal processing at the transmit and the receive side to establish a number of independent communication channels [1]. Usually this requires the antennas inside the array to be spaced sufficiently far apart such that they can obtain substantially different samples of the electromagnetic field. On the other hand, when the antenna separation is small, the field samples are similar and eventually become almost the same as the distance between neighboring antennas decreases further towards zero. As this happens, the wave propagation becomes the same between any pair of transmit and receive antennas, making the two arrays essentially look like single antennas. The arrays can no longer distinguish between different directions, which makes multistreaming with very compact antenna arrays impossible [2].

This standard argument from the signal processing literature ignores, however, the electromagnetic interaction of antennas with each other and the electromagnetic field. This interaction causes a number of interesting effects to occur which are important for the multistreaming capability. The electromagnetic field is *changed* by the presence of the electric currents flowing in the antenna [3]. Also, *coupling* occurs between the otherwise independent sources of *noise* inside the receiver front-ends [4]. Moreover, the noise received by the antenna array in an isotropic background noise environment is necessarily *correlated* when the antennas are place close to each other [5]. Moreover, *impedance matching* networks which are connected between the antenna ports and the inputs of the low-noise amplifiers, or the outputs of the high power amplifiers impact the properties of the system. When all these effects are taken into account and made use of by proper engineering, it turns out that multistreaming may still work well even with compact antenna arrays. We demonstrate this by analyzing a 2×2-MIMO system of half-wavelength dipoles and matching networks in a simple multipath environment consisting of two metallic reflection plates. Circuit theoretic multiport analysis shows that in the absence of heat loss the multistreaming capability can be maintained even when the distance between neighboring antennas in the array approaches zero.

*Notation*. In this paper, we use bold lower-case letters for vectors and bold upper-case letters for matrices. The expectation operation is denoted by $\mathrm{E}[\cdot]$, while $^*$, $^{\mathrm{T}}$, and $^{\mathrm{H}}$, are the complex conjugate, the transposition, and the complex conjugate transposition, respectively. Moreover, $\|\cdot\|_{\mathrm{F}}$, denotes the Frobenius norm, and $\mathbf{I}_n$, and $\mathbf{O}_n$, are the $n$-dimensional identity and zero matrices, respectively. Finally, $\mathrm{Re}\{\cdot\}$, and $\mathrm{Im}\{\cdot\}$ denote the real-part and imaginary-part, respectively.

## II. System under Consideration

Consider two antenna arrays shown in Figure 1, each composed of two thin and lossless half wavelength dipoles. One array is used for transmission the other for reception. The dipoles are oriented in the same direction, say parallel to the

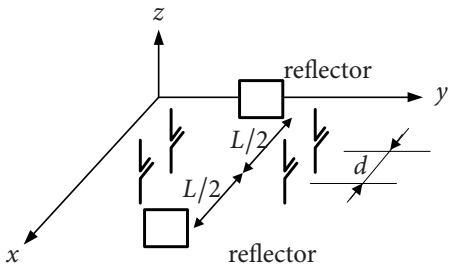


Figure 1: Transmission system under consideration.

$z$-axis. There are two ideal metallic reflection plates placed in the middle between the two arrays and oriented parallel to the $y$-$z$-plane. These reflectors ensure that there is multipath transmission and reception, which is necessary to successfully employ multistreaming. What is not shown in Figure 1 are the

978-1-61284-074-1/11/$26.00 ©2011 IEEE

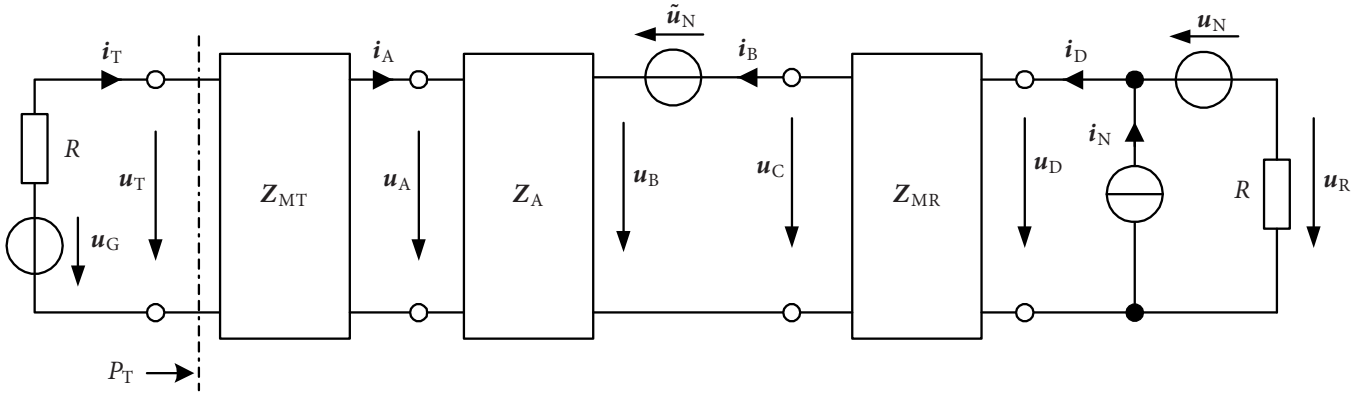


Figure 2: Multiport model of a MIMO communication system, comprising (from left to right) high-power amplifiers, transmit impedance matching network, noisy antenna multiport, receive impedance matching network, and low-noise amplifiers.

high power amplifiers (HPA), the low-noise amplifiers (LNA) and the two lossless impedance matching networks, which are connected between these amplifiers and the antenna ports at each end of the link, respectively. In order to analyze the information theoretic properties of this communication system, we have to model the interactions between all these components, namely the amplifiers, the matching networks, the antennas and the reflectors. We are going to do this by a circuit theoretic multiport approach. This will lead us to an information theoretic system model which captures all the relevant interactions consistently with the governing physics.

## III. Multiport System Model

The circuit theoretic multiport model of the the 2×2-MIMO system under consideration is shown in Figure 2. It consist of the following elements.

### A. High-power Amplifiers

The HPAs are assumed to be linear and modeled as ideal voltage sources with a series resistance $R$. The open-circuit generator voltage vector $\boldsymbol{u}_G \in \mathbb{C}^{2\times 1} \cdot \mathrm{V}$ contains the information that we want to transfer to the receiver.

### B. Transmit Impedance Matching Network

The generators are connected to an impedance matching network which operation is described by:

$$\begin{bmatrix} \boldsymbol{u}_T \\ \boldsymbol{u}_A \end{bmatrix} = \boldsymbol{Z}_{MT} \begin{bmatrix} \boldsymbol{i}_T \\ -\boldsymbol{i}_A \end{bmatrix}, \tag{1}$$

where $\boldsymbol{Z}_{MT} \in \mathbb{C}^{4\times 4} \cdot \Omega$ is its impedance matrix, and the port voltage vectors $\boldsymbol{u}_T$, $\boldsymbol{u}_A \in \mathbb{C}^{2\times 1} \cdot \mathrm{V}$, and the corresponding port current vectors $\boldsymbol{i}_T, \boldsymbol{i}_A \in \mathbb{C}^{2\times 1} \cdot \mathrm{A}$ are defined in Figure 2. We assume that the transmit impedance matching network is *reciprocal* and *lossless*, which necessitates that $\boldsymbol{Z}_{MT}$ is a *symmetric matrix with vanishing real-part* [6].

### C. The Noiseless Antenna Multiport

Modeling the coupling between all pairs of the four antennas is taken care of by the antenna multiport, described by:

$$\begin{bmatrix} \boldsymbol{u}_A \\ \boldsymbol{u}_B \end{bmatrix} = \boldsymbol{Z}_A \begin{bmatrix} \boldsymbol{i}_A \\ \boldsymbol{i}_B \end{bmatrix} = \begin{bmatrix} \boldsymbol{Z}_{AT} & \boldsymbol{Z}_{ATR} \\ \boldsymbol{Z}_{ART} & \boldsymbol{Z}_{AR} \end{bmatrix} \begin{bmatrix} \boldsymbol{i}_A \\ \boldsymbol{i}_B \end{bmatrix}, \tag{2}$$

where $\boldsymbol{Z}_A \in \mathbb{C}^{4\times 4} \cdot \Omega$ is its impedance matrix which is composed of the *transmit impedance matrix* $\boldsymbol{Z}_{AT} \in \mathbb{C}^{2\times 2} \cdot \Omega$, that describes the mutual coupling between the transmit side antennas, the *receive impedance matrix* $\boldsymbol{Z}_{AR} \in \mathbb{C}^{2\times 2} \cdot \Omega$, which describes the mutual coupling between the receive side antennas, and finally, the *transimpedance matrix* $\boldsymbol{Z}_{ART} \in \mathbb{C}^{2\times 2} \cdot \Omega$, that described the mutual coupling between each pair of transmit and receive side antennas. Because antennas are reciprocal [3], there is $\boldsymbol{Z}_A = \boldsymbol{Z}_A^{\mathrm{T}}$, which means that $\boldsymbol{Z}_{ATR} = \boldsymbol{Z}_{ART}^{\mathrm{T}}$, and that both $\boldsymbol{Z}_{AT}$ and $\boldsymbol{Z}_{AR}$ are symmetric matrices.

### D. Isotropic Antenna Noise

The impedance matrix $\boldsymbol{Z}_A$ only describes a noiseless antenna array. In reality, even lossless antennas are noisy due to the reception of background noise. When this background noise impinges on the receive side antenna array *isotropically*, it can be shown that the *open-circuit* antenna noise voltage vector $\tilde{\boldsymbol{u}}_N \in \mathbb{C}^{2\times 1} \cdot \mathrm{V}$, has the following correlation matrix [5]:

$$\mathrm{E}\left[\tilde{\boldsymbol{u}}_N \tilde{\boldsymbol{u}}_N^{\mathrm{H}}\right] = 4\mathrm{k}T_A \Delta f \, \mathrm{Re}\{\boldsymbol{Z}_{AR}\}, \tag{3}$$

where k is Boltzmann's constant, $T_A$ is the *noise temperature* of the antenna, and $\Delta f$ is the bandwidth. In the general case, where the background noise is non-isotropic, the correlation matrix of the open-circuit noise voltage depends both on the spatial distribution of the impinging background noise power density and on the radiation characteristics of the employed antennas. In the following, we focus on *isotropic* background noise and work with the correlation matrix given in (3).

### E. Receive Impedance Matching Network

The noisy antenna ports are connected to one side of another impedance matching network, described by:

$$\begin{bmatrix} \boldsymbol{u}_D \\ \boldsymbol{u}_C \end{bmatrix} = \boldsymbol{Z}_{MR} \begin{bmatrix} \boldsymbol{i}_D \\ -\boldsymbol{i}_B \end{bmatrix}, \tag{4}$$

where $\boldsymbol{Z}_{MR} \in \mathbb{C}^{4\times 4} \cdot \Omega$ is its impedance matrix, and the port voltage vectors $\boldsymbol{u}_C$, $\boldsymbol{u}_D \in \mathbb{C}^{2\times 1} \cdot \mathrm{V}$, and the corresponding port current vectors $\boldsymbol{i}_B, \boldsymbol{i}_D \in \mathbb{C}^{2\times 1} \cdot \mathrm{A}$ are defined in Figure 2. We assume that the receive impedance matching network is *reciprocal* and *lossless*, which necessitates that $\boldsymbol{Z}_{MR}$ is a *symmetric matrix with vanishing real-part* [6].

### F. Low-Noise Amplifiers

The noise contributions of the LNAs can be modeled by inclusion of both a voltage noise $\boldsymbol{u}_{\mathrm{N}} \in \mathbb{C}^{2\times 1} \cdot \mathrm{V}$, and a current noise $\boldsymbol{i}_{\mathrm{N}} \in \mathbb{C}^{2\times 1} \cdot \mathrm{A}$, [7]. This is shown in the right-most part of Figure 2. We assume that the noise contributions of the two LNAs are uncorrelated, which is reasonable when the LNAs are independent devices. However, the noise voltage and the noise current corresponding to each LNA are usually correlated. Hence, we obtain the following stochastic properties:

$$\left.\begin{aligned} \mathrm{E}\big[\boldsymbol{i}_{\mathrm{N}}\boldsymbol{i}_{\mathrm{N}}^{\mathrm{H}}\big] &= \beta\,\mathbf{I}_2, \\ \mathrm{E}\big[\boldsymbol{u}_{\mathrm{N}}\boldsymbol{u}_{\mathrm{N}}^{\mathrm{H}}\big] &= \beta R_{\mathrm{N}}^2\,\mathbf{I}_2, \\ \mathrm{E}\big[\boldsymbol{u}_{\mathrm{N}}\boldsymbol{i}_{\mathrm{N}}^{\mathrm{H}}\big] &= \rho\beta R_{\mathrm{N}}\,\mathbf{I}_2. \end{aligned}\right\} \tag{5}$$

Note that $\beta \in \mathbb{R}_+ \cdot \mathrm{A}^2$ is the second moment of the noise current within a bandwidth $\Delta f$. From the first and second line of (5), we see that

$$R_{\mathrm{N}} = \sqrt{\mathrm{E}\big[|u_{\mathrm{N},j}|^2\big] \,/\, \mathrm{E}\big[|i_{\mathrm{N},j}|^2\big]}, \quad j \in \{1,2\}, \tag{6}$$

is the so-called *noise-resistance* of the LNAs. From (6) and the first and last line of (5) we see that

$$\rho = \frac{\mathrm{E}\big[u_{\mathrm{N},j}\, i_{\mathrm{N},j}^*\big]}{\sqrt{\mathrm{E}\big[|u_{\mathrm{N},j}|^2\big] \cdot \mathrm{E}\big[|i_{\mathrm{N},j}|^2\big]}}, \quad j \in \{1,2\}, \tag{7}$$

which is the *complex noise correlation coefficient* of the LNAs.

### G. Unilateral Approximation

While it is true in general that in the equation (2), we have $\boldsymbol{Z}_{\mathrm{ATR}} = \boldsymbol{Z}_{\mathrm{ART}}^{\mathrm{T}}$, it is also true that in radio communications the signal attenuation between the transmitter and the receiver is usually extremely large. Hence, $\|\boldsymbol{Z}_{\mathrm{ATR}}\|_{\mathrm{F}} = \|\boldsymbol{Z}_{\mathrm{ART}}\|_{\mathrm{F}} \ll \|\boldsymbol{Z}_{\mathrm{AT}}\|_{\mathrm{F}}$ holds true in practice. This motivates to keep $\boldsymbol{Z}_{\mathrm{ART}}$ as it is, but to set $\boldsymbol{Z}_{\mathrm{ATR}} = \mathbf{O}_2$ in (2):

$$\begin{bmatrix} \boldsymbol{u}_{\mathrm{A}} \\ \boldsymbol{u}_{\mathrm{B}} \end{bmatrix} \approx \begin{bmatrix} \boldsymbol{Z}_{\mathrm{AT}} & \mathbf{O}_2 \\ \boldsymbol{Z}_{\mathrm{ART}} & \boldsymbol{Z}_{\mathrm{AR}} \end{bmatrix} \begin{bmatrix} \boldsymbol{i}_{\mathrm{A}} \\ \boldsymbol{i}_{\mathrm{B}} \end{bmatrix}. \tag{8}$$

The expression (8) will be called the *unilateral approximation*. Because $\boldsymbol{u}_{\mathrm{A}} \approx \boldsymbol{Z}_{\mathrm{AT}}\boldsymbol{i}_{\mathrm{A}}$, the electrical properties at the transmit side antenna ports are (almost) independent of what happens at the receiver. This significantly simplifies analysis of the communication system and synthesis of some of its parts (for example, the impedance matching networks). In order not to disrupt the presentation of the material, we postpone the discussion on when the unilateral approximation is actually justified to Section VII. Meanwhile, we assume that the approximate equality in (8) can be though of being an exact one for all practical purposes.

## IV. Decoupling the Antenna Ports

In the noiseless case, the cascade made of the antenna multiport and the two impedance matching networks can be described (within the realm of the unilateral approximation) as:

$$\left.\begin{bmatrix} \boldsymbol{u}_{\mathrm{T}} \\ \boldsymbol{u}_{\mathrm{D}} \end{bmatrix}\right|_{\tilde{\boldsymbol{u}}_{\mathrm{N}} = \mathbf{0}} = \begin{bmatrix} \boldsymbol{Z}_{\mathrm{T}} & \mathbf{O}_2 \\ \boldsymbol{Z}_{\mathrm{RT}} & \boldsymbol{Z}_{\mathrm{R}} \end{bmatrix} \begin{bmatrix} \boldsymbol{i}_{\mathrm{T}} \\ \boldsymbol{i}_{\mathrm{D}} \end{bmatrix}. \tag{9}$$

The transmit impedance matching network can be designed such that in (9):

$$\boldsymbol{Z}_{\mathrm{T}} = R\,\mathbf{I}_2 \tag{10}$$

holds true. This means that the *antenna ports at the transmit side array are decoupled* and each of them just looks like a resistance of value $R$. This ensures that each generator sees a matched load, thus enabling it to transfer maximum power to the antenna array independently of the voltage of the other generator. By circuit analysis of the multiport model in Figure 2 using the unilateral approximation (8), it is fairly straight forward an exercise to show that a transmit impedance matching network with the impedance matrix:

$$\boldsymbol{Z}_{\mathrm{MT}} = \begin{bmatrix} \mathbf{O}_2 & -\mathrm{j}\sqrt{R}\,\mathrm{Re}\{\boldsymbol{Z}_{\mathrm{AT}}\}^{1/2} \\ -\mathrm{j}\sqrt{R}\,\mathrm{Re}\{\boldsymbol{Z}_{\mathrm{AT}}\}^{1/2} & -\mathrm{j}\,\mathrm{Im}\{\boldsymbol{Z}_{\mathrm{AT}}\} \end{bmatrix}, \tag{11}$$

indeed ensures that (10) holds true. Herein, j represents the imaginary unit ($\mathrm{j}^2 = -1$), and the notation $\boldsymbol{A}^{1/2}$ is used to mean any matrix square root of $\boldsymbol{A}$, that is, any matrix which, when multiplied with itself, gives $\boldsymbol{A}$. Note that $\boldsymbol{Z}_{\mathrm{MT}}$ from (11) is a symmetric matrix with vanishing real-part, such that it really describes a reciprocal and lossless multiport. In a similar fashion, one can design the receive impedance matching network such that it has an impedance matrix given by:

$$\boldsymbol{Z}_{\mathrm{MR}} = \begin{bmatrix} \mathrm{j}\,\mathrm{Im}\{Z_{\mathrm{out}}\}\,\mathbf{I}_2 & \mathrm{j}\sqrt{\mathrm{Re}\{Z_{\mathrm{out}}\}}\,\mathrm{Re}\{\boldsymbol{Z}_{\mathrm{AR}}\}^{1/2} \\ \mathrm{j}\sqrt{\mathrm{Re}\{Z_{\mathrm{out}}\}}\,\mathrm{Re}\{\boldsymbol{Z}_{\mathrm{AR}}\}^{1/2} & -\mathrm{j}\,\mathrm{Im}\{\boldsymbol{Z}_{\mathrm{AR}}\} \end{bmatrix}, \tag{12}$$

which leads in (9) to

$$\boldsymbol{Z}_{\mathrm{R}} = Z_{\mathrm{out}}\,\mathbf{I}_2. \tag{13}$$

Thus, the *receiver side antenna ports are electrically decoupled* and each provides a source with impedance $Z_{\mathrm{out}} \in \mathbb{C} \cdot \Omega$ to the inputs of the LNAs. While the choice $Z_{\mathrm{out}} = R$ ensures that the receiver extracts maximum power from the antennas, a better signal to noise ratio (SNR) usually can be achieved by choosing $Z_{\mathrm{out}}$ differently. We will come back to this point in a moment.

The impedance matching networks, of course, have impact on the effective transimpedance $Z_{\mathrm{RT}}$ in (9). It turns out from circuit analysis of the multiport model in Figure 2, that the specific choice of the transmit and receive impedance matching networks according to (11) and (12) leads to the effective transimpedance matrix:

$$\boldsymbol{Z}_{\mathrm{RT}} = \sqrt{R \cdot \mathrm{Re}\{Z_{\mathrm{out}}\}}\,\mathrm{Re}\{\boldsymbol{Z}_{\mathrm{AR}}\}^{-1/2}\,\boldsymbol{Z}_{\mathrm{ART}}\,\mathrm{Re}\{\boldsymbol{Z}_{\mathrm{AT}}\}^{-1/2}. \tag{14}$$

While the impedance matching networks have done their job to decoupled the receiver's ports and the transmitter's ports, the mutual coupling *within* both arrays (in terms of $\mathrm{Re}\{\boldsymbol{Z}_{\mathrm{AR}}\}$ and $\mathrm{Re}\{\boldsymbol{Z}_{\mathrm{AT}}\}$), has reappeared by modifying the coupling *between* the transmitter and the receiver. By virtue of (14), the transimpedance $\boldsymbol{Z}_{\mathrm{ART}}$ of the antenna multiport is turned into the effective transimpedance $\boldsymbol{Z}_{\mathrm{RT}}$ of the cascade of the antenna multiport and the two impedance matching networks. We will see later that it is precisely the transformation (14) which is responsible for allowing effective multi-streaming even with compact antenna arrays.

## V. Minimizing Noise Figure

Let us now return to the problem of determining the optimum value for $Z_{\text{out}}$. Circuit analysis of the multiport in Figure 2, given the impedance matching networks from (11) and (12), reveals that the noise contaminated observable $\boldsymbol{u}_{\text{R}} \in \mathbb{C}^{2\times 1} \cdot \text{V}$ is given by:

$$\boldsymbol{u}_{\text{R}} = \frac{½}{R + Z_{\text{out}}} \boldsymbol{Z}_{\text{RT}} \boldsymbol{u}_{\text{G}} + \boldsymbol{n}, \tag{15}$$

where $\boldsymbol{n} \in \mathbb{C}^{2\times 1} \cdot \text{V}$ is the resulting noise voltage with

$$\text{E}\left[\boldsymbol{n}\boldsymbol{n}^{\text{H}}\right] = \sigma_n^2 \mathbf{I}_2, \tag{16}$$

with

$$\sigma_n^2 = \frac{\beta R^2}{|R + Z_{\text{out}}|^2} \left( |Z_{\text{out}}|^2 - 2R_{\text{N}} \text{Re}\{\rho^* Z_{\text{out}}\} + R_{\text{N}}^2 + \right. \\ \left. + \frac{4\text{k}T_{\text{A}}\Delta f}{\beta} \text{Re}\{Z_{\text{out}}\} \right). \tag{17}$$

It is interesting enough that the resulting noise is *uncorrelated* between the two observables $u_{\text{R},1}$ and $u_{\text{R},2}$, which constitute $\boldsymbol{u}_{\text{R}}$. The reason for this behavior is twofold. Firstly, because the receive impedance matching network decouples the receiver's antenna ports, the noise contributions of the two LNAs do *not* mix. Secondly, it is due to the background noise received by the antennas being *isotropic*. Recall that this makes the open-circuit noise voltage of the antenna have the correlation matrix given in (3). Now what happens is that an open-circuit noise voltage with exactly this correlation matrix, becomes decorrelated by the very same receive impedance matching network that decouples the receiver's antenna ports.

Let us now compute the signal to noise ratio $\text{SNR}_j$ at the $j$-th observable, defined by:

$$\text{SNR}_j = \frac{\text{E}\left[|u_{\text{R},j}|^2 \mid \boldsymbol{n} = \mathbf{0}\right]}{\text{E}\left[|u_{\text{R},j}|^2 \mid \boldsymbol{u}_{\text{G}} = \mathbf{0}\right]}, \quad j \in \{1, 2\}. \tag{18}$$

To this end, it is handy to express $\text{SNR}_j$ as the ratio:

$$\text{SNR}_j = \frac{\text{SNR}_j^{\text{avail}}}{\text{NF}_j}, \quad j \in \{1, 2\}, \tag{19}$$

where $\text{SNR}_j^{\text{avail}}$ is the so-called *available* SNR which would result if the LNAs were noiseless:

$$\text{SNR}_j^{\text{avail}} = \text{SNR}_j\big|_{\beta=0}, \quad j \in \{1, 2\}, \tag{20}$$

and the factor $\text{NF}_j$ is the famous *noise figure*. Thus, the noise figure is the factor by which the LNAs' noise contribution reduces the available SNR. Substituting (15) into (18), and the latter into (19), it follows with the help of (16), (17) and (20):

$$\text{NF}_j = \text{NF} = 1 + \frac{|Z_{\text{out}}|^2 - 2R_{\text{N}} \text{Re}\{\rho^* Z_{\text{out}}\} + R_{\text{N}}^2}{4\text{k}T_{\text{A}}\Delta f \, \text{Re}\{Z_{\text{out}}\} / \beta}. \tag{21}$$

Note that the noise figure does *not* depend on $j$, hence, both LNAs have the same noise figure. Moreover, NF is a function of $Z_{\text{out}}$, which can be chosen such that NF is *minimized*. Performing the straight forward minimization of (21) with respect to $Z_{\text{out}}$, it turns out that the unique solution is given by:

$$Z_{\text{opt}} = R_{\text{N}} \cdot \left( \sqrt{1 - (\text{Im}\{\rho\})^2} + \text{j} \cdot \text{Im}\{\rho\} \right). \tag{22}$$

Note that $|Z_{\text{opt}}| = R_{\text{N}}$. Substituting this $Z_{\text{opt}}$ for $Z_{\text{out}}$ in (21) then shows that the minimum noise figure is given by:

$$\text{NF}_{\text{min}} = 1 + \frac{\beta R_{\text{N}}}{2\text{k}T_{\text{A}}\Delta f} \cdot \left( \sqrt{1 - (\text{Im}\{\rho\})^2} - \text{Re}\{\rho\} \right). \tag{23}$$

Substituting (22) into (17), we find with the help of (23) that:

$$\sigma_n^2 = \frac{R^2 R_{\text{N}}}{|R + Z_{\text{opt}}|^2} \sqrt{1 - (\text{Im}\{\rho\})^2} \, 4\text{k}T_{\text{A}}\Delta f \, \text{NF}_{\text{min}}. \tag{24}$$

## VI. The MIMO Channel Matrix

It is reasonable to define *transmit power* $P_{\text{T}}$ as the total electric power which is delivered by the generators into the transmit impedance matching network, as indicated on the left hand side of Figure 2. Thus,

$$P_{\text{T}} = \text{E}\left[\text{Re}\left\{\boldsymbol{u}_{\text{T}}^{\text{H}} \boldsymbol{i}_{\text{T}}\right\}\right]. \tag{25}$$

From (9), we have $\boldsymbol{u}_{\text{T}} = \boldsymbol{Z}_{\text{T}} \boldsymbol{i}_{\text{T}}$, and the transmit impedance matching network ensures that $\boldsymbol{Z}_{\text{T}} = R\mathbf{I}_2$. The latter also implies that $\boldsymbol{u}_{\text{T}} = ½\boldsymbol{u}_{\text{G}}$, and so we can write (25) as:

$$P_{\text{T}} = \frac{1}{4R} \text{E}\left[\|\boldsymbol{u}_{\text{G}}\|_2^2\right]. \tag{26}$$

Now, it is convenient to define a scaled version of the generator voltage vector $\boldsymbol{u}_{\text{G}}$ as the *channel input vector:* $\boldsymbol{x}$, and a scaled version of the noisy observation $\boldsymbol{u}_{\text{R}}$ as the *channel output vector:* $\boldsymbol{y}$:

$$\boldsymbol{x} = \frac{1}{2\sqrt{R}} \boldsymbol{u}_{\text{G}}, \quad \boldsymbol{y} = \frac{|R + Z_{\text{opt}}|}{R\sqrt{R_{\text{N}}\sqrt{1 - (\text{Im}\{\rho\})^2}}} \boldsymbol{u}_{\text{R}}. \tag{27}$$

Applying (27) to (15), it follows with the help of (14) and (24):

$$\boldsymbol{y} = \tilde{\boldsymbol{H}}\boldsymbol{x} + \boldsymbol{\vartheta}, \tag{28}$$

where $\boldsymbol{\vartheta}$ contains noise samples with correlation matrix:

$$\text{E}\left[\boldsymbol{\vartheta}\boldsymbol{\vartheta}^{\text{H}}\right] = \sigma_\vartheta^2 \mathbf{I}_2, \quad \sigma_\vartheta^2 = 4\text{k}T_{\text{A}}\Delta f \, \text{NF}_{\text{min}}, \tag{29}$$

hence, samples of *white* noise. Moreover, the transmit power equals

$$P_{\text{T}} = \text{E}\left[\|\boldsymbol{x}\|_2^2\right], \tag{30}$$

and is, thus, the mean squared Euclidean norm of the channel input vector $\boldsymbol{x}$. In this way, (28) is a standard MIMO system model, with the MIMO channel matrix $\tilde{\boldsymbol{H}} \in \mathbb{C}^{2\times 2}$ given by:

$$\tilde{\boldsymbol{H}} = \text{e}^{-\text{j}\varphi} \, \text{Re}\{\boldsymbol{Z}_{\text{AR}}\}^{-1/2} \, \boldsymbol{Z}_{\text{ART}} \, \text{Re}\{\boldsymbol{Z}_{\text{AT}}\}^{-1/2}, \tag{31}$$

where $\varphi = \text{angle}\left(R + Z_{\text{opt}}\right)$. Clearly, the unimodular constant term $\text{e}^{-\text{j}\varphi}$ has no impact on performance, so that it can safely be neglected in information theory, replacing $\tilde{\boldsymbol{H}}$ by:

$$\boldsymbol{H} = \text{Re}\{\boldsymbol{Z}_{\text{AR}}\}^{-1/2} \, \boldsymbol{Z}_{\text{ART}} \, \text{Re}\{\boldsymbol{Z}_{\text{AT}}\}^{-1/2}. \tag{32}$$

A beautiful aspect of this result is that, from an information theory perspective, there is *no* need to know any of the internal details, such as $R$, $R_{\text{N}}$, $\rho$, and $Z_{\text{opt}}$. All that matters is condensed into the channel matrix given in (32), and can be obtained *solely* and readily from parts of the array impedance matrix $\boldsymbol{Z}_{\text{A}}$. In other words, pay attention to $\boldsymbol{Z}_{\text{A}}$!

## VII. Justification of the Unilateral Approximation

The result (32) builds on the validity of the unilateral approximation (8) and (9). From the latter follows that

$$\boldsymbol{u}_{\mathrm{T}} \approx \boldsymbol{Z}_{\mathrm{T}} \boldsymbol{i}_{\mathrm{T}}, \tag{33}$$

which means that the presence of the receiver does not influence the electric situation at the transmitter in any appreciable amount. In order to check to what extent this is actually true, we change (9) into:

$$\left[\begin{array}{c} \boldsymbol{u}_{\mathrm{T}} \\ \boldsymbol{u}_{\mathrm{D}} \end{array}\right]\Bigg|_{\tilde{\boldsymbol{u}}_{\mathrm{N}} = \boldsymbol{0}} \approx \left[\begin{array}{cc} \boldsymbol{Z}_{\mathrm{T}} & \boldsymbol{Z}_{\mathrm{RT}}^{\mathrm{T}} \\ \boldsymbol{Z}_{\mathrm{RT}} & \boldsymbol{Z}_{\mathrm{R}} \end{array}\right]\left[\begin{array}{c} \boldsymbol{i}_{\mathrm{T}} \\ \boldsymbol{i}_{\mathrm{D}} \end{array}\right], \tag{34}$$

which is a better approximation than is (9), for the system actually *is* reciprocal. From (34) then follows in the noise-free case (where $\boldsymbol{u}_{\mathrm{D}} = -R\boldsymbol{i}_{\mathrm{D}}$):

$$\boldsymbol{u}_{\mathrm{T}} \approx \left(\boldsymbol{Z}_{\mathrm{T}} - \boldsymbol{Z}_{\mathrm{RT}}^{\mathrm{T}} \left(R\mathbf{I}_2 + \boldsymbol{Z}_{\mathrm{R}}\right)^{-1} \boldsymbol{Z}_{\mathrm{RT}}\right) \boldsymbol{i}_{\mathrm{T}}. \tag{35}$$

The idea is that as long as there is no appreciable difference between the predictions (33) and (35), the action of the receiver on the transmitter is negligible. Therefore, the unilateral approximation is justified as long as

$$\max_{\boldsymbol{i}_{\mathrm{T}}} \sqrt{\frac{\|\boldsymbol{Z}_{\mathrm{RT}}^{\mathrm{T}} \left(R\mathbf{I}_2 + \boldsymbol{Z}_{\mathrm{R}}\right)^{-1} \boldsymbol{Z}_{\mathrm{RT}} \boldsymbol{i}_{\mathrm{T}}\|_2^2}{\|\boldsymbol{Z}_{\mathrm{T}} \boldsymbol{i}_{\mathrm{T}}\|_2^2}} \ll 1 \tag{36}$$

holds true, for then the difference in prediction of the transmitter port voltages from (33) and (35) is guaranteed to be relatively small. The maximization in (36) is a generalized eigenvalue problem so that the condition can be restated as:

$$\max \ \mathrm{SV}\left\{\boldsymbol{Z}_{\mathrm{RT}}^{\mathrm{T}} \left(R\mathbf{I}_2 + \boldsymbol{Z}_{\mathrm{R}}\right)^{-1} \boldsymbol{Z}_{\mathrm{RT}} \boldsymbol{Z}_{\mathrm{T}}^{-1}\right\} \ll 1, \tag{37}$$

where $\mathrm{SV}\{\cdot\}$ denotes the singular values of its argument. Substituting (10), (13) and (14) into (37), then shows with the help of (32) that

$$\max \ \mathrm{SV}\left\{\boldsymbol{H}^{\mathrm{T}}\boldsymbol{H}\right\} \ll \frac{|R + Z_{\mathrm{opt}}|}{\mathrm{Re}\left\{Z_{\mathrm{opt}}\right\}} \tag{38}$$

must hold true for the unilateral approximation to be applicable. Since in praxi both $R > 0$, and $\mathrm{Re}\{Z_{\mathrm{opt}}\} > 0$, and

$$\frac{|R + Z_{\mathrm{opt}}|}{\mathrm{Re}\left\{Z_{\mathrm{opt}}\right\}} \geq 1, \quad \text{for } R > 0, \ \mathrm{Re}\left\{Z_{\mathrm{opt}}\right\} > 0,$$

the right hand side of (38) is lower bounded by unity. Thus, the condition for the applicability of the result (32) for the channel matrix $\boldsymbol{H}$ simplifies to:

$$\max \ \mathrm{SV}\left\{\boldsymbol{H}^{\mathrm{T}}\boldsymbol{H}\right\} \ll 1. \tag{39}$$

The condition $\max \mathrm{SV}\{\boldsymbol{H}^{\mathrm{T}}\boldsymbol{H}\} < 0.01$, should be sufficient for all practical purposes. Note that the condition (39) can always be fulfilled by moving the receiver and transmitter sufficiently far apart, as the elements of $\boldsymbol{H}$ decrease their magnitude (on average) with increasing distance. We will elaborate on this important point in Section IX.

## VIII. The Array Impedance Matrix

We have developed enough theory to approach the problem of computing the MIMO channel matrix for the scenario from Figure 1. To do this, we need to know the array impedance matrix $\boldsymbol{Z}_{\mathrm{A}}$, or more precisely, the real-parts of $\boldsymbol{Z}_{\mathrm{AT}}$ and $\boldsymbol{Z}_{\mathrm{AR}}$ (which are identical here, because identical antenna arrays are used at transmitter and receiver), and the transimpedance matrix $\boldsymbol{Z}_{\mathrm{ART}}$.

### A. Two $\lambda/2$-dipoles in the Far-field

Let us begin with a single half-wavelength dipole in the origin O of a Cartesian coordinate system and lined up with its $z$-axis. With a current $i$ flowing through the dipole's excitation port, the resulting electric field at a point P in the *far-field* is given in spherical coordinates as (e.g., [8], page 153):

$$\vec{\boldsymbol{E}} = \vec{\boldsymbol{e}}_{\theta} \, \frac{\mathrm{j}i\mathrm{e}^{-\mathrm{j}2\pi r/\lambda}}{2\pi r \epsilon_0 c} \cdot \frac{\cos\left(\tfrac{1}{2}\pi\cos\theta\right)}{\sin\theta}, \tag{40}$$

where $\lambda$ is the wave length, $r$ the distance of the point to the origin, and $\theta$ the angle that $\overline{\mathrm{OP}}$ makes with the $z$-axis. Moreover, $\epsilon_0$ is the electric constant, and $c$ is the speed of light. Now let the point P be in the $x$-$y$-plane, such that $\theta = \pi/2$. If another $\lambda/2$-dipole is located in P and oriented in parallel to the first dipole (i.e., in the direction of the $z$-axis), then the open-circuit voltage that is induced into this dipole is given by the product of the electric field strength and the dipole's effective length $l_{\mathrm{eff}}$ (e.g., [8], page 80). Because $l_{\mathrm{eff}} = \lambda/\pi$ for a $\lambda/2$ dipole (e.g., [3], page 509), the transimpedance of these two dipoles equals:

$$Z_{\mathrm{ART}} = \frac{\mathrm{e}^{-\mathrm{j}2\pi r/\lambda}}{r} \cdot \frac{\mathrm{j}\lambda}{2\pi^2 \epsilon_0 c}, \quad r \gg \lambda. \tag{41}$$

### B. Inter- and Intra-Array Mutual Coupling

Consider now the top-view of the scenario from Figure 1 (looking from an elevated position down into the direction of the negative $z$-axis) as shown in Figure 3. The four filled circles

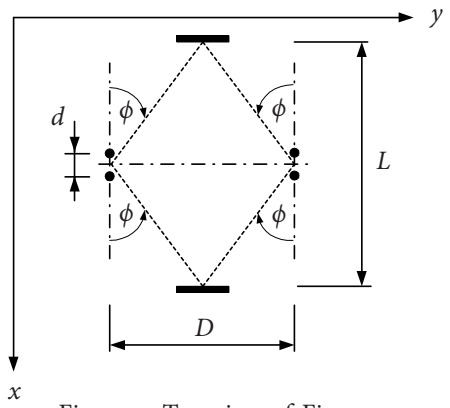


Figure 3: Top-view of Figure 1.

are the thin wires of the four dipoles seen straight from the top. The transmitter's and the receiver's array are separated by the distance $D$, while the two $\lambda/2$-dipoles inside each array are spaced a distance $d$ apart. Two symmetrically located metallic reflection plates provide a defined multi-path environment.

They are set a distance $L$ apart. When a line were drawn from the center of each array to the center of each reflection plate, it would make an angle $\phi$ with the array line-ups (parallel to the $x$-axis). From plane geometry, we have that

$$L = D/\tan\phi. \tag{42}$$

The distance $D$ is assumed to be large enough such that the partner array and the reflectors are well in the far field. We assume in the following that the wave propagation can be approximated accurately enough by quasi optical rays with perfect reflections. Because there are three paths (a direct path and two paths over the reflection plates) by which the transmitter can reach the receiver, the transimpedance matrix $\boldsymbol{Z}_{\mathrm{ART}}$ can be written as the sum of three components:

$$\boldsymbol{Z}_{\mathrm{ART}} = \boldsymbol{Z}_{\mathrm{ART},1} + \boldsymbol{Z}_{\mathrm{ART},2} + \boldsymbol{Z}_{\mathrm{ART},3} \tag{43}$$

where (applying (41) for each pair of distant antennas)

$$\boldsymbol{Z}_{\mathrm{ART},1} = \frac{\alpha \mathrm{e}^{-\mathrm{j}2\pi D/\lambda}}{D}\begin{bmatrix}1 & 1\\ 1 & 1\end{bmatrix}, \quad \text{with } \alpha = \frac{\mathrm{j}\lambda}{2\pi^2\epsilon_0 c}, \tag{44}$$

corresponds to the direct path, and

$$\boldsymbol{Z}_{\mathrm{ART},2,3} = \frac{-\alpha \mathrm{e}^{-\mathrm{j}2\pi r/\lambda}}{r}\begin{bmatrix}\mathrm{e}^{\pm\mathrm{j}2\pi\frac{d}{\lambda}\cos\phi} & 1\\ 1 & \mathrm{e}^{\mp\mathrm{j}2\pi\frac{d}{\lambda}\cos\phi}\end{bmatrix} \tag{45}$$

correspond to the paths over the two reflection plates, respectively. Herein, $r$ is the distance the waves have to travel from the center of the transmitter's array to the center of the receiver's array, taking the longer way over the reflection plates:

$$r = D/\sin\phi. \tag{46}$$

The negative sign of the factor $\alpha$ in (45) is due to the reflected waves having to change their phase by 180 degrees, because the incident field is polarized *tangential* to the reflectors. Using the relationship $D/r = \sin\phi$ from (46), we can rewrite (43) as:

$$\boldsymbol{Z}_{\mathrm{ART}} = \frac{\alpha \mathrm{e}^{-\mathrm{j}2\pi D/\lambda}}{D}\begin{bmatrix}\tilde{a} & \tilde{b}\\ \tilde{b} & \tilde{a}\end{bmatrix}, \quad \begin{aligned}\tilde{a} &= 1 - 2\mathrm{e}^{-\mathrm{j}\Psi}\sin(\phi)\cos(2\pi\tfrac{d}{\lambda}\cos\phi)\\ \tilde{b} &= 1 - 2\mathrm{e}^{-\mathrm{j}\Psi}\sin\phi,\end{aligned} \tag{47}$$

where we have introduced the variable

$$\Psi = \frac{2\pi D}{\lambda}\left(\frac{1}{\sin\phi} - 1\right), \tag{48}$$

for notational convenience. Now what happens when the distance $d$ of the dipoles inside the arrays is made smaller and smaller? It is clear from (47) that $\boldsymbol{Z}_{\mathrm{ART}}$ will tend to become a rank one matrix:

$$\lim_{d\to 0}\boldsymbol{Z}_{\mathrm{ART}} = \frac{\alpha \mathrm{e}^{-\mathrm{j}kD}}{D}\left(1 - 2\mathrm{e}^{-\mathrm{j}\Psi}\sin\phi\right)\begin{bmatrix}1 & 1\\ 1 & 1\end{bmatrix}. \tag{49}$$

Because of this it is usually argued that by making $d$ smaller and smaller, the two antennas in each array essentially look like a single antenna, making multi-streaming more and more difficult, and ultimately impossible as $d \to 0$. However, recall from Section VI, that from an information theory point of view, it is *not* $\boldsymbol{Z}_{\mathrm{ART}}$ which is the relevant MIMO channel matrix, but rather the matrix $\boldsymbol{H}$ given in (32). Therefore, in order to find $\boldsymbol{H}$, we also have to find the real-parts of the transmit and receive array impedance matrices, which account for the mutual coupling of the antennas *within* the arrays (intra-array coupling), in addition to $\boldsymbol{Z}_{\mathrm{ART}}$, which describes the mutual coupling *between* the arrays (inter-array coupling). Now it is an interesting fact that the real-part of the normalized array impedance matrix (normalized such that the main diagonal is unity) for two co-linear $\lambda/2$-dipoles is almost exactly the same as the normalized array impedance matrix of two Hertzian dipoles [9]. One therefore obtains: [9], [10]:

$$\mathrm{Re}\{\boldsymbol{Z}_{\mathrm{AT}}\} = \mathrm{Re}\{\boldsymbol{Z}_{\mathrm{AR}}\} = 73\Omega\begin{bmatrix}1 & \Theta(2\pi d/\lambda)\\ \Theta(2\pi d/\lambda) & 1\end{bmatrix}, \tag{50}$$

where

$$\Theta(x) = \frac{3}{2}\left(\frac{\sin x}{x} + \frac{\cos x}{x^2} - \frac{\sin x}{x^3}\right). \tag{51}$$

Notice that as $d \to 0$, the rank of these impedance matrices becomes unity. Because in (32), these matrices appear with their *inverse* square root, it is possible that the channel matrix $\boldsymbol{H}$ *retains full rank,* despite that $\boldsymbol{Z}_{\mathrm{ART}}$, $\mathrm{Re}\{\boldsymbol{Z}_{\mathrm{AT}}\}$, and $\mathrm{Re}\{\boldsymbol{Z}_{\mathrm{AR}}\}$ all tend to rank-deficient matrices. Let us look now into this.

## IX. Super-Compact MIMO System

By substituting (51) into (50) and the latter together with (47) into (32), one can calculate the actual MIMO channel matrix $\boldsymbol{H}$. To this end, one can make use of the fact that:

$$\begin{bmatrix}1 & \Theta\\ \Theta & 1\end{bmatrix}^{-1/2}\begin{bmatrix}\tilde{a} & \tilde{b}\\ \tilde{b} & \tilde{a}\end{bmatrix}\begin{bmatrix}1 & \Theta\\ \Theta & 1\end{bmatrix}^{-1/2} = \frac{1}{1-\Theta^2}\begin{bmatrix}\tilde{a}-\tilde{b}\Theta & \tilde{b}-\tilde{a}\Theta\\ \tilde{b}-\tilde{a}\Theta & \tilde{a}-\tilde{b}\Theta\end{bmatrix}. \tag{52}$$

Asymptotically, for $d \to 0$, one obtains a *super-compact* MIMO system with channel matrix:

$$\boldsymbol{H}_0 = \lim_{d\to 0}\boldsymbol{H} = \gamma\begin{bmatrix}a & b\\ b & a\end{bmatrix}, \quad \begin{aligned}a &= 4\mathrm{e}^{\mathrm{j}\Psi} - 3\sin(\phi) + 5\sin 3\phi\\ b &= 4\mathrm{e}^{\mathrm{j}\Psi} - 13\sin(\phi) - 5\sin 3\phi,\end{aligned} \tag{53}$$

where

$$\gamma = \frac{\mathrm{j}1.64\mathrm{e}^{-\mathrm{j}2\pi D/\lambda}}{2\pi D/\lambda}\cdot\frac{\mathrm{e}^{-\mathrm{j}\Psi}}{8}. \tag{54}$$

As $\det\boldsymbol{H}_0 = \gamma^2 80\left(\mathrm{e}^{\mathrm{j}\Psi} - 2\sin\phi\right)(\sin(\phi) + \sin 3\phi)$, we can see that, in general, $\boldsymbol{H}_0$ *has full rank which makes multi-streaming possible even for arbitrarily small antenna separation d inside the arrays.*

In order to obtain more insight we should look at the eigenvalues of $\boldsymbol{H}_0^{\mathrm{H}}\boldsymbol{H}_0$, for they are directly related to the information theoretic channel capacity [1].

$$\boldsymbol{H}_0^{\mathrm{H}}\boldsymbol{H}_0 = \boldsymbol{V}\begin{bmatrix}\xi_1 & 0\\ 0 & \xi_2\end{bmatrix}\boldsymbol{V}^{\mathrm{H}}. \tag{55}$$

The eigenvalues $\xi_1$ and $\xi_2$ compute to:

$$\left.\begin{aligned}\xi_1 &= |\gamma|^2 64\left(3 - 2\cos(2\phi) - 4\cos(\Psi)\sin\phi\right),\\ \xi_2 &= |\gamma|^2 1600\cos^4(\phi)\sin^2\phi.\end{aligned}\right\} \tag{56}$$

Of course, it is good to have as large eigenvalues as possible, so that from (56) we see that $\Psi$ should be chosen such that $\cos\Psi = -1$, because $\sin\phi \geq 0$. Hence:

$$\Psi_{\mathrm{opt}} = \pi + n\cdot 2\pi, \quad n \in \{0, \pm 1, \pm 2, \cdots\}. \tag{57}$$

Substituting $\Psi_{\text{opt}}$ for $\Psi$ in (56), it turns out that $\xi_1 > \xi_2$. Hence, we obtain for the eigenvalue ratio:

$$\frac{\xi_{\min}}{\xi_{\max}} = \frac{\xi_2}{\xi_1} = 25\frac{\cos^4(\phi)\sin^2\phi}{(1+2\sin\phi)^2} < 1. \tag{58}$$

Effective multistreaming requires that both these eigenvalues are similar, for otherwise the system supports one »strong« and one »weak« data stream. The weak data stream, contributing only marginally to the total channel capacity, would make multistreaming much less effective. Because $\xi_{\min}/\xi_{\max} < 1$, it is clear that the ideal case of having identical eigenvalues does not happen for the super-compact MIMO system under consideration. However, one can bring the ratio $\xi_{\min}/\xi_{\max}$ as close to unity as possible by maximization with respect to the angle $\phi$. Taking the first derivative of (58) with respect to $\phi$ and setting it to zero, we find that the optimum $\phi$ must be a solution of:

$$\cos^2(\phi) - 2\sin^2(\phi)(1+2\sin\phi) = 0. \tag{59}$$

Substituting $\tau = \sin\phi$ turns (59) into:

$$4\tau^3 + 3\tau^2 - 1 = 0.$$

From its three roots only one is real-valued. Using this root, we therefore obtain:

$$\phi_{\text{opt}} = \arcsin\left(\tfrac{1}{4}\left(-1 + \left(7-4\sqrt{3}\right)^{1/3} + \left(7+4\sqrt{3}\right)^{1/3}\right)\right). \tag{60}$$

For we can restrict $\phi$ to the range $0 < \phi < \pi/2$ (see Figure 3), the function $\sin(\phi)$ is strictly monotonic. As a consequence, the optimum solution is *unique*, and given numerically as:

$$\phi_{\text{opt}} \approx 27^\circ. \tag{61}$$

By letting $\Psi = \Psi_{\text{opt}}$, and $\phi = \phi_{\text{opt}}$, it follows with (48) and (57) that the optimum distance $D_{\text{opt}}$ is given by

$$D_{\text{opt}} = \lambda\frac{n+\tfrac{1}{2}}{-1+1/\sin\phi_{\text{opt}}}. \tag{62}$$

Using the numerical value for $\phi_{\text{opt}}$, we obtain

$$D_{\text{opt}} \approx 0.836\lambda\cdot(n+\tfrac{1}{2}), \quad n\in\mathbb{N}, \quad n \gg 1. \tag{63}$$

Finally, we can also give the optimum distance $L$ between the reflectors with the help of (42) explicitly:

$$L_{\text{opt}} = D_{\text{opt}}/\tan\phi_{\text{opt}} \approx 1.955\cdot D_{\text{opt}}. \tag{64}$$

When $\phi = \phi_{\text{opt}}$, we obtain from (58) that

$$\max\frac{\xi_{\min}}{\xi_{\max}} \approx 0.892. \tag{65}$$

This ratio of the eigenvalues of $\boldsymbol{H}_0^{\text{H}}\boldsymbol{H}_0$ is very close to unity. In fact, $\xi_{\min}$ is less than 0.5 dB below $\xi_{\max}$. This means that *effective multistreaming is possible even if the antenna separation inside the arrays approaches zero.*

Recall that all developed results rely on the validity of the unilateral approximation. In Section VII, we have developed a criterion which allows this validity to be checked by evaluating (39). Substituting in (53) $\Psi = \Psi_{\text{opt}}$ from (57), one obtains:

$$\max\ \text{SV}\left\{\boldsymbol{H}_0^{\text{T}}\boldsymbol{H}_0\right\} = 64|\gamma|^2(1+2\sin\phi)^2 \le 576|\gamma|^2. \tag{66}$$

Requiring that $\max \text{SV}\left\{\boldsymbol{H}^{\text{T}}\boldsymbol{H}\right\} < 0.01$, it follows with (54) that

$$D > 7.9\lambda \tag{67}$$

ensures that the unilateral approximation is applicable *for any placement of the reflectors,* that is, for any angle $\phi$. This means, that in (63), we have to make sure that $n \ge 9$. For the optimum placement of the reflectors ($\phi = \phi_{\text{opt}}$), the unilateral approximation is already justified if $D > 5\lambda$.

## X. Compact MIMO System

While the asymptotic analysis where we let $d \to 0$ is interesting and insightful, a real MIMO system will always have finite $d$. In the following, we therefore have a look at the system from Figure 1 with variable distance $d$. The solid curve in Figure 4 shows the quantity

$$\Psi = \max_{\phi}\frac{\xi_{\min}}{\xi_{\max}},$$

as a function of $d/\lambda$. One can spot a number of interesting observations. For a relatively large antenna separation, characterized by $d > 0.82\lambda$, there always is some way or other to place the reflection plates which result in a unity $\Psi$. This represents the best use of multistreaming because two streams can be supported with *perfectly equal* share of the total channel capacity. Now when we reduce $d$ below $0.82\lambda$, we see that $\Psi$ begins to drop until it reaches its global minimum of $\Psi_{\min} \approx 0.45$ at an antenna separation of about $0.61\lambda$. It is quite remarkable that a relatively large separation of $d = 0.61\lambda$ is the worst case with respect to multistream transmission, where even the best placing of the reflection plates will result in more than 3 dB eigenvalue spread. However, as we decrease the distance $d$ further, remarkably enough, $\Psi$ begins to *increase* again, ultimately reaching the limit of 0.892, as $d \to 0$. In fact, compact arrays, with $d \le 0.25\lambda$, can allow for remarkably effective multistream operation.

The dashed curve in Figure 4 shows the hypothetical result for $\Psi$ for the case where the intra-array coupling, i.e., mutual coupling between antennas inside the arrays, is ignored. This can be calculated by merely setting the real-parts of $\boldsymbol{Z}_{\text{AT}}$ and $\boldsymbol{Z}_{\text{AR}}$ equal to scaled identity matrices, irrespective of the antenna separation $d$. This ignorance of intra-array coupling is commonplace in contemporary signal processing and information theory literature [2]. Without considering intra-array coupling the results for $\Psi$ are remarkably different. Once $d$ is reduced below $\lambda/2$, the hypothetical value of $\Psi$ drops monotonically towards zero as $d$ is reduced. This is in striking contrast to the large value of $\Psi$ which actually results from taking the full antenna mutual coupling into account. Moreover, ignoring intra-array coupling does not predict the actual low value of $\Psi$ for the relatively large separation of $d = 0.61\lambda$, thereby predicting falsely that $\Psi$ is unity for $d \ge \lambda/2$. This demonstrates how important it is to take the full mutual antenna coupling into account not only for compact antenna arrays (where strong near-field interaction is almost obvious), but also – and especially so – for arrays with an antenna separation in the neighborhood of $\lambda/2$ – the darling distance in signal processing literature.

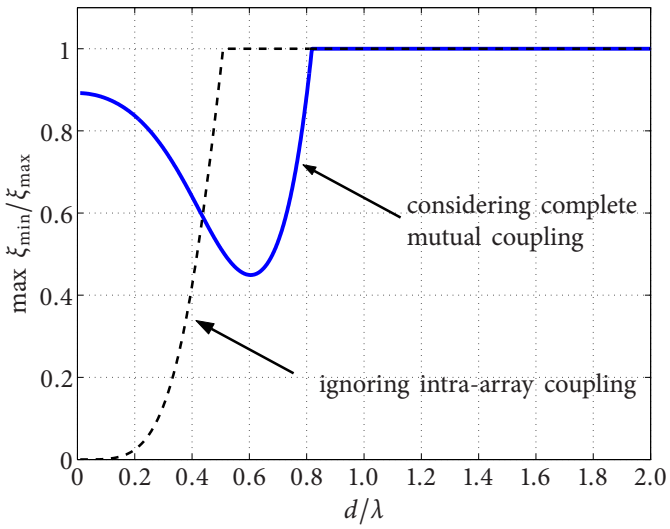


Figure 4: Smallest achievable eigenvalue spread of $\boldsymbol{H}^{\mathrm{H}}\boldsymbol{H}$.

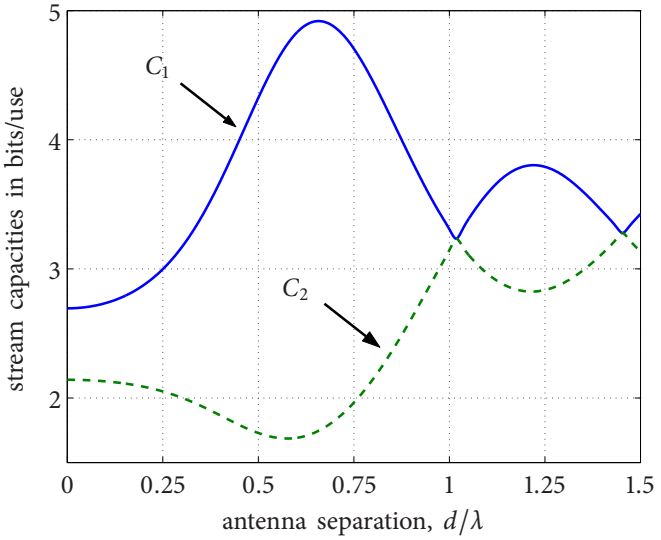


Figure 5: Stream capacities vs. antenna separation.

Of course, the smallest eigenvalue spread $\Psi$ does not tell the whole story about multistreaming. For a more complete picture it is beneficial to also study the channel capacity itself. For a given MIMO channel matrix $\boldsymbol{H} \in \mathbb{C}^{2\times 2}$, one can compute the channel capacity as:

$$C = C_1 + C_2, \tag{68}$$

where $C_1$ and $C_2$ are the capacities for the first and the second data stream, respectively. Assuming that the total transmit power $P_{\mathrm{T}}$ is shared equally between these two streams, the stream capacities $C_1$ and $C_2$ can be computed as [1]:

$$C_j = \log_2\Big(1 + P_{\mathrm{T}}\,\xi_j/(2\sigma_\vartheta^2)\Big), \quad j \in \{1, 2\}, \tag{69}$$

where $\xi_1 \geq \xi_2$ are the ordered eigenvalues of $\boldsymbol{H}^{\mathrm{H}}\boldsymbol{H}$, and $\sigma_\vartheta^2$ is the effective noise power defined in (29).

The stream capacities are shown in Figure 5, as a function of the antenna separation $d$ per wavelength $\lambda$, for some *fixed* value of transmit power. For each value of $d/\lambda$, the two reflection plates are shifted (that is, the angle $\phi$ is changed) until the *largest* sum capacity $C_1 + C_2$ is reached. Knowing the previous result of the investigation of the eigenvalue spread, it might not come as a complete surprise to see that the capacity $C_2$ of the weaker stream does *not* break down as $d/\lambda$ approaches zero. On the contrary, as $d$ is decreased from about $0.58\lambda$, the capacity for the weaker stream actually increases. In fact, for small values of $d/\lambda$ it contributes a substantial amount (about 44%) to the sum capacity $C_1 + C_2$.

## XI. Outlook

The obtained results for super-compact arrays (where $d \to 0$) heavily rely on the assumption that there is no heat loss in the system (neither in the impedance matching networks, nor in the antenna wires). Heat loss presents additional noise contributions which set a lower limit to the useful antenna separation $d$. Because most of the heat-loss related noise is likely to result from within the impedance matching networks, the results depend on its internal structure. Further research is needed in this area.

Another effect which sets a lower limit on the useful antenna separation is the bandwidth of the impedance matching networks and the antenna array, for both tend to reduce as $d$ shrinks. Design of broadband matching networks in the context of compact antenna arrays is still a completely open research problem. Among first steps in this direction might be an attempt to identify suitable circuit structures for broadband low-loss matching networks and look for possibilities to implement part of their functionality by the antenna array itself.

## XII. Conclusion

From a circuit theoretic multiport analysis which captures all relevant physics of mutual antenna coupling we have shown for a 2×2-MIMO system with four half-wavelength dipoles and two reflectors in empty space, that in the absence of heat loss effective multistreaming remains possible even for arbitrarily small antenna separation inside the arrays.

## References


[1] I. E. Telatar, "Capacity of Multi-Antenna Gaussian Channels," *European Transactions on Telecommunications*, vol. 10(6), pp. 585–596, nov 1999.

[2] D. Tse and P. Viswanath, *Fundamentals of Wireless Communication*. Cambridge University Press, 2005.

[3] S. A. Schelkunoff and H. T. Friis, *Antennas. Theory and Practice*. New York, NY: Wiley, 1952.

[4] M. T. Ivrlač and J. A. Nossek, "Toward a Circuit Theory of Communication," *IEEE Transactions on Circuits and Systems I: Regular Papers*, vol. 57(7), pp. 1663–1683, 2010.

[5] R. Q. Twiss, "Nyquist's and Thevenin's Theorems Generalized for Nonreciprocal Linear Networks," *J. Appl. Phys.*, vol. 26, pp. 599–602, May 1955.

[6] V. Belevitch, *Classical Circuit Theory*. Holden Day, San Francisco, 1968.

[7] H. Hillbrand and P. Russer, "An Efficient Method for Computer Aided Noise Analysis of Linear Amplifier Networks," *IEEE Transactions on Circuits and Systems*, vol. 23(4), pp. 235–238, jun 1976.

[8] A. Balanis, *Antenna Theory*. Second Edition, John Wiley & Sons, 1997.

[9] M. T. Ivrlač, "Lecture Notes on Circuit Theory and Communications (unpublished)," *Technische Universität München*, May 2010.

[10] H. Yordanov, M. T. Ivrlač, P. Russer, and J. A. Nossek, "Arrays of Isotropic Radiators — A Field-theoretic Justification," in *Proc. of the IEEE/ITG International Workshop on Smart Antennas, 2009*, Berlin, Germany, feb 2009.